Check for updates

Decreased cingulo-opercular network functional connectivity mediates the impact of aging on visual processing speed

Adriana L. Ruiz-Rizzo [a,b,*], Christian Sorg [a,c], Natan Napiórkowski [a,b], Julia Neitzel [a,b], Aurore Menegaux [a,b], Hermann J. Müller [a,b], Signe Vangkilde [d], Kathrin Finke [a,e]

[a] Department of General and Experimental Psychology, Ludwig-Maximilans-Universität München, Munich, Germany
[b] Graduate School of Systemic Neurosciences, GSN LMU Munich, Munich, Germany
[c] TUM-Neuroimaging Center, TUM-NIC, Technische Universität München, Munich, Germany
[d] Department of Psychology, Center for Visual Cognition, University of Copenhagen, Copenhagen, Denmark
[e] Hans Berger Department of Neurology, Jena University Hospital, Jena, Germany

ARTICLE INFO

ABSTRACT

The neural factors that account for the visual processing speed reduction in aging are incompletely understood. Based on previous reports of age-related decreases in the intrinsic functional connectivity (iFC) within the cingulo-opercular network and its relevance for processing speed, we hypothesized that these decreases are associated with age-related reductions in visual processing speed. We used a whole-report task and modeling based on Bundesen's "theory of visual attention" to parameterize visual processing speed in 91 healthy participants aged from 20 to 77 years. iFC was estimated using independent component analysis of resting-state functional magnetic resonance imaging data. From the clusters within the cingulo-opercular network exhibiting age-related decreased iFC, we found a cluster in the left insula to be particularly associated with visual processing speed and to mediate the age effect on visual speed. This mediation was not observed for age-related decreased iFC in other networks or for other attentional parameters. Our results point to the iFC in the cingulo-opercular network, represented by the left insula, as being a relevant marker for visual processing speed changes in aging.

© 2018 Elsevier Inc. All rights reserved.

1. Introduction

A decline in processing speed represents a fundamental aspect of cognitive aging (Salthouse, 1996). In particular, a reduction of visual processing speed, or the rate of information encoding into visual short-term memory (VSTM), has previously been established in both healthy (Espeseth et al., 2014; Habekost et al., 2013; McAvinue et al., 2012; Wiegand et al., 2014) and, more severely, pathological aging (Bublak et al., 2011; Ruiz-Rizzo et al., 2017) using a computational approach based on Bundesen's (1990) "theory of visual attention" (TVA). TVA permits the contribution of visual processing speed to the efficiency of visual selection to be quantitatively estimated, independently of motor speed as well as other visual attention functions such as VSTM capacity or the visual threshold, which also degrade during aging. The TVA-based visual processing speed parameter, C, is estimated from a participant's performance in a psychophysical (letter) whole-report task (Bundesen, 1990; Habekost et al., 2014), where C provides a measure of the individual's rate of visual information uptake in elements (i.e., letters) per second. Although the reduction of visual processing speed is generally thought to be brought about by neural aging, the underlying brain mechanisms are only incompletely understood. In this study, we aimed to shed light on this issue by investigating the role of the cingulo-opercular network in the reduction of visual processing speed as a result of aging.

The cingulo-opercular network, also referred to as a "salience" (e.g., Seeley et al., 2007) or "ventral attention" (e.g., Yeo et al., 2011) network, is centered on the anterior insula and the anterior cingulate cortex (Dosenbach et al., 2007, 2008; Menon and Uddin, 2010; Seeley et al., 2007). It is thought to play a central role in "tonic alertness": the endogenous ability to maintain an appropriate level of arousal (Posner and Petersen, 1990; Sturm and Willmes, 2001). Thus, for instance, the spontaneous activity fluctuations of the cingulo-opercular network, measured using functional magnetic resonance imaging (fMRI), have been shown to correlate with markers of tonic alertness, such as upper alpha band power (Sadaghiani et al., 2010) and pupil size fluctuations (Schneider et al., 2016). Furthermore, the cingulo-opercular network displays sustained activity during perceptual processing

* Corresponding author at: Department of General and Experimental Psychology, Ludwig-Maximilans-Universität München, Leopoldstraße 13, 80802 Munich, Germany. Tel.: +49 89 2180 72569; fax: +49 (0) 89 2180 5211.
E-mail address: adriana.ruiz@lmu.de (A.L. Ruiz-Rizzo).

(Sestieri et al., 2014), with its activity level relating to the speed of stimulus detection (Coste and Kleinschmidt, 2016). Importantly, in the present context, intrinsic functional connectivity (iFC) in the cingulo-opercular network increases with rising demands on tonic alertness (Sadaghiani and D'Esposito, 2015)—where iFC refers to the coherence of the infra-slow (i.e., 0.01−0.1 Hz) spontaneous neural activity, typically measured with BOLD (blood oxygenation level dependent) fMRI during resting state (De Luca et al., 2006; Fox and Raichle, 2007; Raichle, 2015). In fact, tonic alertness has been proposed to relate closely to visual processing speed C (e.g., Bundesen et al., 2015). This is evidenced, for example, by tonic alertness influencing visual processing speed in a TVA-based whole-report task (Matthias et al., 2010). Also, raising tonic alertness through psychostimulant medication increases visual processing speed (Finke et al., 2010). And of note, iFC in the cingulo-opercular network has been found to be related to visual processing speed in healthy young adults (Ruiz-Rizzo et al., 2018).

Age-related decreases of the iFC in the cingulo-opercular network have been reported previously and were found to be related to a reduced global cognitive state (He et al., 2014) and lowered visuospatial and executive abilities (Onoda et al., 2012). Given that a significant amount of variance in diverse cognitive tasks (employed in the previous reports) can be accounted for by visual processing speed especially in old age (e.g., Deary and Stough, 1996), we hypothesized that reduced iFC in the cingulo-opercular network would be particularly associated with a decrease in visual processing speed. Based on the documented associations between age and both reduced iFC in the cingulo-opercular network (He et al., 2014; Onoda et al., 2012) and visual processing speed (Espeseth et al., 2014; Habekost et al., 2013; McAvinue et al., 2012; Wiegand et al., 2014), we further explored whether the reduced iFC would mediate the effect of age on visual processing speed, in a cross-sectional sample of healthy (younger and older) adults.

To investigate the association between iFC in the cingulo-opercular network and the age-related decrease of visual processing speed, we examined whether individuals' iFC would correlate with their visual processing speed C (as estimated from performance in a TVA-based task requiring participants to report as many letters as possible from briefly presented letter arrays [so-called whole-report task]). To assess the concurrent criterion validity of this association, we further examined whether the results would generalize to a clinically well-established measure of visual processing speed: the Trail Making Test, form A (TMT-A; Tombaugh, 2004). To take account of individual differences in the brain size that could influence the relationship between iFC and behavior, the correlations were computed controlling for the brain volume (Smith et al., 2002, 2004). Next, we performed two lines of control analysis. First, we checked whether the association between the cingulo-opercular network and visual processing speed is a specific one, as hypothesized, rather than being part of a more global relationship between changes in iFC and visual attention functions in general. That is, given the well-documented age-related decreases in iFC in the default mode and dorsal-attention networks (see, e.g., Andrews-Hanna et al., 2007; Damoiseaux et al., 2008; Ferreira and Busatto, 2013), age-related reductions in visual processing speed might conceivably be associated with a general age-related decrease of iFC rather than with that of the cingulo-opercular network exclusively. To check for this, (1) we examined whether visual processing speed C also relates to the iFC in other networks, and (2) we assessed whether the iFC in the cingulo-opercular network relates to other visual attention functions previously reported to change with aging, such as the visual perceptual threshold and VSTM storage capacity (see, e.g., McAvinue et al., 2012). Second, we controlled for potentially relevant confounds in

the association between iFC in the cingulo-opercular network and visual processing speed. In particular, given that iFC in the cingulo-opercular network has previously been found to be related to anxiety (see, e.g., Seeley et al., 2007) and anxiety level might in turn affect the processing speed, we controlled for anxiety using the state-trait anxiety inventory (STAI; Laux et al., 1981; Spielberger et al., 1970). Two other potential confounds we controlled for were vascular risk and gray matter density, both of which are influenced by aging and might also affect processing speed (e.g., D'Esposito et al., 2003; Lu et al., 2013). Following these control analyses, we went on to explore whether the iFC in the cingulo-opercular network mediates the well-established relation between age and visual processing speed, as hypothesized.

2. Material and methods

2.1. Participants

The present study included 91 healthy adults in the age range from 20 to 77 years (mean age: 48.8 ± 19.2 years; 46 females; mean education: 12.0 ± 1.6 years; 4 left-handed; Table 1). The study was approved by the Ludwig-Maximilians-University Munich ethics committee, and written informed consent was obtained from all participants. Initially, 108 adults (19−78 year old) of the Munich INDIREA aging cohort[1] took part in the study. The Mini Mental State Examination (MMSE; Folstein et al., 1975) was used for screening for cognitive impairments in participants from 60 years onwards (i.e., an MMSE score below 27), and the Beck Depression Inventory (BDI; Beck et al., 1996) for screening for symptoms of depression in all participants (i.e., a BDI score above 19). Seventeen participants were excluded because they asked to be withdrawn from the study (n = 9) or because of incomplete or unreliable data (n = 3; 1 exhibited significant head motion in the resting-state fMRI session, for 1, TVA-based parameters fitting was inadequate, and 1 had an MMSE score below 27), uncorrected visual acuity decreases (n = 2), or symptoms of depression (n = 3). From the remaining 91 participants, those in the older adults group had no indication of cognitive impairment (mean MMSE score: 29 ± 0.9), and all were free of previous or current psychiatric or neurological disorders, psychiatric or neurological medication, diabetes, color blindness, or current symptoms of depression (mean BDI score: 5.2 ± 4.8). In one session, participants underwent resting-state fMRI at the Department of Neuroradiology, Klinikum rechts der Isar, Munich (Germany). In a separate, psychophysical-testing session, visual attention functioning was assessed using the whole-report task. In the psychophysical-testing session, participants also completed the TMT and MMSE and filled out demographic, anxiety, and BDI questionnaires. Session order depended on individual participants' convenience. The average time between sessions was 2.6 months.

2.2. Assessment and estimation of visual processing speed C

A whole-report task, based on TVA (Bundesen, 1990), was used to estimate visual processing speed C. On each trial, four red letters were briefly presented to participants, who were instructed to verbally report, in any order, all letters they were fairly certain they had seen. Stimuli were randomly chosen from the set of letters (A, B, D, E, F, G, H, J, K, L, M, N, O, P, R, S, T, V, X, Z). Letters were arranged in

---

Table 1
Demographic variables by subgroups of age decades

Age range (y)	N	Sex (F/M)	Education (y)
20–29	22	13/9	12.6 ± 0.6
30–39	11	2/9	12.3 ± 1.2
40–49	14	9/5	12.2 ± 1.0
50–59	11	10/1	11.9 ± 1.2
60–69	11	4/7	11.5 ± 1.5
70–79	22	8/14	11.6 ± 2.6

Mean ± standard deviations (SD) are shown in the last column.
Key: F, female; M, male.

Fig. 1. Example of a trial and the mask used for whole-report task. Symbols were symmetrically presented contralateral to the target stimuli to ensure balanced physical stimulation. Stimuli diameters were equal to 1.3° visual angle.

the form of a semicircle, with a radius of 5.3° of visual angle, on either the right or the left of a central fixation point, as shown in Fig. 1. To ensure balanced visual stimulation in both hemifields, targets were accompanied by four blue symbols (composed of random letter parts; see Fig. 1 for an example) of the same luminance displayed on the semicircle on the other side of fixation. Visual stimuli were 1.3° of the visual angle in diameter, and both letters and symbols appeared only once in a particular trial.

The task included 10 blocks of 40 trials each (400 trials in total), with targets presented in the left and right hemifields, respectively, in half of the blocks. Five individually adjusted stimulus exposure durations were determined in a short pretest and introduced in the subsequent whole-report task. To start with, the participant was presented with one adjustment trial displayed for 80 ms, with stimulus exposure terminated by postdisplay masks (see below). If the participant reported at least one letter correctly, the exposure duration was decreased by 10 ms, and this procedure continued for the next 15 adjustment trials. These (16) adjustment trials were divided into 4 blocks, with each 4 adjustment trials accompanied by 4 trials with displays presented unmasked for 200 ms and 4 trials with postdisplay masks (see below for details) presented for 250 ms (yielding 12 trials per block). The exposure duration was decreased until the (shortest) duration was established at which the participant could no longer report one letter. If this point was reached before the last of the 16 adjustment trials, the exposure duration was kept constant for the few remaining adjustment trials. Setting the exposure duration so short was meant to ensure that we would obtain a valid estimate of the visual perceptual threshold parameter. Then, based on the shortest exposure duration, four longer values were additionally chosen to allow for variability in letter report performance across the whole range from near floor to near ceiling and thus render the TVA-based parameter estimation more precise. On *masked* trials, the displays were shown for one of the five durations and immediately followed by masks (a scattered patch of red and blue squares, 1.3° in size) presented for 900 ms at each stimulus location, so as to avoid visual persistence effects. In addition to trials with masked display exposure, we introduced *unmasked* trials (without postdisplay masks) to increase the variability of *effective* exposure times (by allowing for an additional component of iconic memory buffering; Sperling, 1960) and thus ensure reliable and valid TVA parameter fitting. Specifically, on unmasked trials, displays were presented at one of two exposure durations: one was the same as the second shortest masked duration and the other one was 200 ms[2]. Thus, overall, trial displays were presented for seven *effective* exposure durations, five masked and two unmasked. A block of 40 trials (with hemifield blocked) thus consisted of 15 masked trials, with 3 trials for each of the 5 set
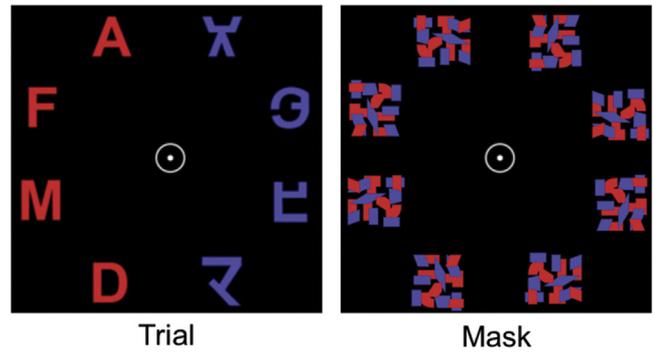
exposure durations; 3 unmasked trials with the second shortest duration; and 22 unmasked trials with 200 ms duration. Trials were presented in a random order within each block.

Participants were tested in a sound-attenuated chamber (Industrial Acoustics Company) with a dim light placed behind them. Stimuli were presented on a 24″ LED screen with an 800px × 600px resolution and a 100-Hz refresh rate. The viewing distance was kept constant at about 65 cm. At the beginning of each block, a black screen with a white arrow appeared pointing toward the side on which the stimuli would appear for that specific block. After stimulus presentation, a white question mark appeared in the center of the screen prompting the start of the verbal report. In each trial, the experimenter entered the reported letters in the reported order and manually started the next trial. The measure of interest was report accuracy (at a given effective exposure duration). At the end of each block, a feedback bar was presented that signaled whether the report accuracy of the actually reported letters ranged between 70% and 90%. If the report accuracy was outside this range, oral instructions were given by the experimenter. If it was above 90%, the participant was told that he or she should try to report more letters, even if not absolutely sure that they are correct. If it dropped below 70%, the participant was told to try to refrain from guessing and report only those letters he/she was relatively sure to have seen. The whole-report task lasted about 45 minutes.

Visual processing speed C was estimated by modeling the participant's report accuracy as a function of the effective exposure duration, using a maximum likelihood-fitting algorithm (Bundesen, 1990; Dyrholm et al., 2011; Kyllingsbaek, 2006). The TVA-based fitting procedure models the probability of correct letter report in terms of an exponential growth function with increasing (effective) exposure duration. The slope of the function at its origin represents the visual processing speed or parameter C, that is, the rate of visual information uptake (in elements per second). In addition, two other parameters were estimated, that in our analyses served for testing whether the relationship between the iFC in the cingulo-opercular network and visual processing speed is a specific one, namely: parameter t_0, indicating the visual perceptual threshold, that is, the longest ineffective exposure duration (in ms) below which information uptake is effectively zero, and parameter K, indicating the maximum number of elements that can be simultaneously represented in VSTM[3]. With aging, t_0 exhibits an increase, whereas K

---

[2] The second shortest was used because the shortest one is too brief for visual perception. A 200-ms unmasked duration was used for the purposes of simultaneous electroencephalographic measurement for the analysis of event-related potentials, which will not be reported here.

[3] An additional parameter, parameter μ, representing the prolongation of the effective exposure duration (in ms) in unmasked trials, was also estimated in the TVA fitting process. However, as μ only serves for the valid estimation of the relevant parameters C, K, and t_0, this parameter is of no further relevance in the present study.

shows a decrease (Espeseth et al., 2014). Critically, the TVA-based estimation of parameter C (visual processing speed) is mathematically independent of that of t_0 and K. Accordingly, the measure of C allows controlling for potential influences of changes in threshold and VSTM storage capacity and has, thus, a high cognitive specificity. In summary, the computational model used had 6 degrees of freedom (df): C, 1 df; t_0, 1 df; K, 3 df (the reported K value is the expected K, given a particular distribution of the probability that, on a given trial, $K = 1, 2, 3,$ or 4); and μ, 1 df. For those participants whose t_0 was estimated to be below 0 (i.e., 11 in total), we refitted the data fixing t_0 at 0[4].

2.3. Paper-and-pencil assessment of visual processing speed: Trail Making Test A

Participants' visual processing speed was also assessed using a standard neuropsychological measure, the TMT-A, to test whether the association between iFC in the cingulo-opercular network and the age-induced reduction in visual processing speed can also be shown when an established paper-and-pencil task is used. The TMT-A[5] measures visual scanning speed in terms of the time required to connect circles with numbers in the ascending order (Reitan and Wolfson, 1985; Tombaugh, 2004) and is widely used in Alzheimer's disease screening batteries (e.g., Weintraub et al., 2009). We examined the association of the time to complete the TMT-A with the iFC of the cingulo-opercular network.

2.4. State-trait anxiety inventory

Given previously reported associations between the iFC in the cingulo-opercular network and anxiety, we also assessed anxiety in our sample and used it as an additional control variable. The STAI Form X (Laux et al., 1981; Spielberger et al., 1970) consists of two (Barnes et al., 2002) self-report scales of 20 items each that measure state and trait anxiety.

2.5. MRI data acquisition

MRI data were acquired on a Philips Ingenia 3T system (Netherlands), using a 32-channel SENSE head coil. Functional MRI T2*-weighted data were collected for 12.5 minutes while participants' rested with their eyes closed, after having been told not to fall asleep. We checked that participants had not fallen asleep by directly asking them immediately after finishing the sequence. Foam padding was used to constrain participants' head motion while scanning, and earplugs and headphones were provided to reduce adverse effects of scanner noise. Six hundred volumes of BOLD-fMRI signal were acquired from each individual, using a multiband (Feinberg and Setsompop, 2013) echo-planar imaging sequence, with a 2-fold in-plane SENSE acceleration (SENSE factor, S = 2) and an M-factor of 2 (Preibisch et al., 2015). Other fMRI acquisition parameters were repetition time = 1250 ms; time to echo = 30 ms; phase encoding direction: anterior-posterior; flip angle = 70°; field of view = 192 mm^2; matrix size = 64 × 64, 40 slices; slice thickness = 3.0 mm; interslice gap 0.3 mm; reconstructed voxel size = 3 × 3 ×

3.29 mm^3. A high-resolution T1-weighted anatomical volume was acquired using a 3D magnetization prepared rapid acquisition gradient echo sequence with the following parameters: repetition time = 9 ms; time to echo = 4 ms; inversion time, TI = 0 ms; flip angle = 8°; 170 sagittal slices; field of view = 240 mm^2; matrix size = 240 × 240; reconstructed voxel size = 1 mm isotropic.

2.6. MRI data analysis

2.6.1. Resting-state fMRI data preprocessing

Six hundred resting-state fMRI volumes per individual were preprocessed using the Data Processing Assistant for Resting-State fMRI (Chao-Gan and Yu-Feng, 2010), a toolbox for data analysis of resting-state fMRI based on MATLAB (R2016b; MathWorks Inc; Natick, MA, USA). To start with, the first five volumes were discarded to compensate for T1 saturation effects. Next, the data were slice-timing corrected, realigned, reoriented to the anterior commissure-posterior commissure axis, and coregistered to the individual structural images. Nuisance variables (i.e., six head motion parameters, white matter, CSF, and global signals) were regressed out from the functional data. Data were normalized to MNI (Montreal Neurological Institute) space with a 2-mm isotropic voxel size and smoothed using a 4-mm full width at half maximum Gaussian kernel (Chao-Gan and Yu-Feng, 2010). Given the relevance of controlling the signal-to-noise ratio in studies of aging (D'Esposito et al., 2003), we examined the temporal signal-to-noise ratio of the fMRI time series (Murphy et al., 2007) in relation to age, but found no significant association [r(89) = −0.07, $p = 0.528$]. The mean framewise displacement values (Power et al., 2012) were used as a control variable in the statistical analyses.

2.6.2. Independent component analysis and dual regression

The preprocessed resting-state fMRI data were analyzed by using probabilistic independent component analysis (ICA) with 20 dimensions in FSL MELODIC (Beckmann and Smith, 2004; Smith et al., 2004), following previous ICA-based studies (e.g., Onoda et al., 2012; Ruiz-Rizzo et al., 2018; Smith et al., 2009). Group ICA permits the identification of spatiotemporal signals representing intrinsic brain networks, besides signals reflecting physiological noise or scanner-related artifacts (Nickerson et al., 2017). The preprocessed data were normalized for voxelwise mean and variance and then reduced to a 20-dimensional subspace by probabilistic principal component analysis. Subsequently, data were decomposed into time courses and spatial maps by optimizing for non-Gaussian spatial distributions using a fixed-point iteration technique (Hyvarinen, 1999). Next, we performed dual regression (Beckmann et al., 2009; Filippini et al., 2009) using these 20 components as input.

Dual regression is a multivariate approach that yields individual spatial maps with associated time courses and works in two stages, namely, a spatial and a temporal regression. First, in the spatial regression, the group-independent component maps obtained from ICA are regressed onto each participant's preprocessed data set, resulting in one time course per component that is further normalized by its standard deviation (Nickerson et al., 2017). Second, in the temporal regression, the time courses obtained are regressed again onto each participant's data set, thus resulting in one spatial map per component. Because these spatial maps can accurately localize differences in the shape (i.e., spatial pattern) and amplitude (i.e., normalized time course) of a particular network (see, e.g., Nickerson et al., 2017), they can be used for the group-level statistical analyses. Next, we selected the components that represented the networks on which we would conduct the group-level statistical analyses.

---

[4] Crucially, when the data of these 11 participants are refitted without the limitation of t_0 being at minimum 0, the mean change in C values was 2.12 (±2.62). Post hoc analyses showed that constraining the model to t_0 at a minimum of 0 does not impact the conclusions of our study or its validity.

[5] We particularly chose the TMT-A because it provides a more straight measure of speed, whereas the TMT-B is supposed to measure executive functions (e.g., task switching).

2.6.3. Network selection

To select the components of interest, we performed a spatial cross-correlation between all the 20 independent components and the templates of the 7-network parcellation reported by Yeo et al. (2011), using the *fslcc* command in FSL. We identified as the cingulo-opercular network the component with the highest spatial correlation coefficient with the "ventral attention" network of Yeo et al. (2011) (component 7, r = 0.23; see Introduction for different naming). We similarly identified the default mode and dorsal-attention networks (component 2, r = 0.25, and component 8, r = 0.30, respectively). Other templates obtained from parcellations similar to ours (i.e., ICA; Allen et al., 2011) further confirmed our selection (cingulo-opercular with IC55_salience of Allen et al.: r = 0.43; default mode with IC53_posterior_default_mode: r = 0.39; and dorsal attention with IC34_attention_left, r = 0.41).

2.7. Statistical analyses

2.7.1. Multiple regression analysis of age on iFC in the cingulo-opercular network

To replicate the age-related decrease in iFC in the cingulo-opercular network (e.g., He et al., 2014; Onoda et al., 2012), we carried out a voxelwise linear regression analysis. We did so because, based on our data-driven approach (i.e., ICA and dual regression), not all voxels within the cingulo-opercular network of each participant equally represent the ICA-derived group cingulo-opercular network (see, e.g., Smith et al., 2014). Each voxel's iFC value (i.e., Z-value) represents how much its time course resembles the network's time course relative to all the other voxels within an individual's brain. Therefore, the inferences that we derive from our results will remain at the network level.

The voxelwise regression of age on the iFC in the cingulo-opercular network, conducted using SPM12 (http://www.fil.ion.ucl.ac.uk/spm/), included participants' education, mean volume-to-volume head motion (i.e., framewise displacement), and sex as regressors of no interest. We repeated this analysis, once on the iFC in the default mode network and once on the iFC in the dorsal-attention network to later assess the specificity of the role of the cingulo-opercular network for visual processing speed C. Clusters were considered significant at $p < 0.05$ familywise error (FWE) corrected for multiple comparisons at the cluster level (height voxelwise threshold $p < 0.001$).

2.7.2. Partial correlation of iFC clusters affected by age with visual processing speed and control measures

Next, we extracted the eigenvariate (i.e., average iFC values) of the significant age-related clusters from a sphere 5 mm in radius around the peak, to examine iFC in relation to the visual processing speed C estimates. This analysis was supplemented by the respective analysis with the paper-and-pencil TMT-A visual processing-speed task. To control the specificity, the eigenvariate was additionally examined in relation to the other visual attention parameters (i.e., VSTM storage capacity, K, and perceptual threshold, t_0), and to anxiety (i.e., STAI) scores. In all these analyses, partial correlations were conducted using participants' brain volume to account for individual differences in the brain size that could influence the relationship between iFC and behavior (see Supplementary Material for details on the estimation of brain volume; Smith et al., 2004, 2002). All reported p values are based on two-tailed tests, unless otherwise specified.

2.7.3. Analysis of a mediating effect of the iFC in the cingulo-opercular network in the relationship between age and visual processing speed decline

Based on previous reports of associations between age and visual processing speed (e.g., McAvinue et al., 2012), between iFC in the cingulo-opercular network in young adults (Ruiz-Rizzo et al., 2018), and between age, iFC in the cingulo-opercular network, and cognitive functioning (e.g., He et al., 2014; Onoda et al., 2012), we hypothesized that the iFC in the cingulo-opercular network might mediate the association between age and visual processing speed. Accordingly, we examined for such a role of the cingulo-opercular network iFC by conducting a mediation analysis. First, the total effect of age on visual processing speed was estimated with a simple linear regression. Second, this total effect was deconstructed into an indirect effect—through the iFC in the cingulo-opercular network—and a direct effect. Third, the indirect effect, reflecting the significance of the mediation, was evaluated using bootstrap confidence intervals (Hayes, 2012; Hayes and Rockwood, 2017; Mackinnon and Fairchild, 2009; Preacher and Hayes, 2004) at 95% level of confidence and based on 10,000 replication samples. The indirect effect represents an estimate of the amount of change in visual processing speed per year of age.

3. Results

3.1. Visual processing speed in aging

Means and standard deviations of TVA parameter visual processing speed C obtained from the whole-report task as well as duration to complete TMT-A are listed in Table 2. Males and females did not differ in these measures (both p-values > 0.445). As expected (e.g., McAvinue et al., 2012), both measures were significantly correlated with age. Finally, and also as expected, both measures were significantly correlated [$r(88) = -0.28$, $p = 0.008$; one young participant lacked TMT-A data], with higher visual processing speed C being associated with less time needed to complete the TMT-A.

3.2. Functional connectivity in the cingulo-opercular network in aging

The cingulo-opercular network encompassed frontal regions including the inferior frontal and middle frontal gyri bilaterally, anterior and middle cingulate cortices; insular regions; the superior temporal gyrus; parietal regions including supramarginal gyrus, inferior parietal lobule, and precuneus; and subcortical regions including the basal ganglia, thalamus, amygdala, brain stem, and cerebellum (one-sample t-test, $p < 0.05$ FWE corrected at the cluster level; Fig. 2).

In a voxelwise multiple regression analysis, we found significantly reduced iFC in the right anterior and bilateral middle cingulate cortices, left insula, right middle frontal gyrus, left cerebellum, and the right posterior medial and left superior frontal gyri with increasing age (controlled for the individual mean volume-to-volume head motion, gender, and education, $p < 0.05$ FWE corrected at the cluster level; Fig. 3 and Table 3).

Table 2
Behavioral results and their correlation with age

Behavioral measure	Mean ± SD	Range	Correlation with age
TVA estimates			
Visual processing speed C	22.52 ± 7.76	9.71—47.00	**r = -0.21 (p = 0.049)**
VSTM capacity K	3.17 ± 0.41	1.95—3.88	**r = -0.25 (p = 0.017)**
Perceptual threshold t_0	13.54 ± 13.76	0.00—67.13	r = 0.19 (p = 0.064)
Trail Making Test A			
TMT-A (s)	32.52 ± 12.99	13.44—74.98	**r = 0.65 (p < 0.001)**

Bold indicates significance at $p < 0.05$, two-tailed.
Key: TVA, theory of visual attention; VSTM, visual short-term memory.
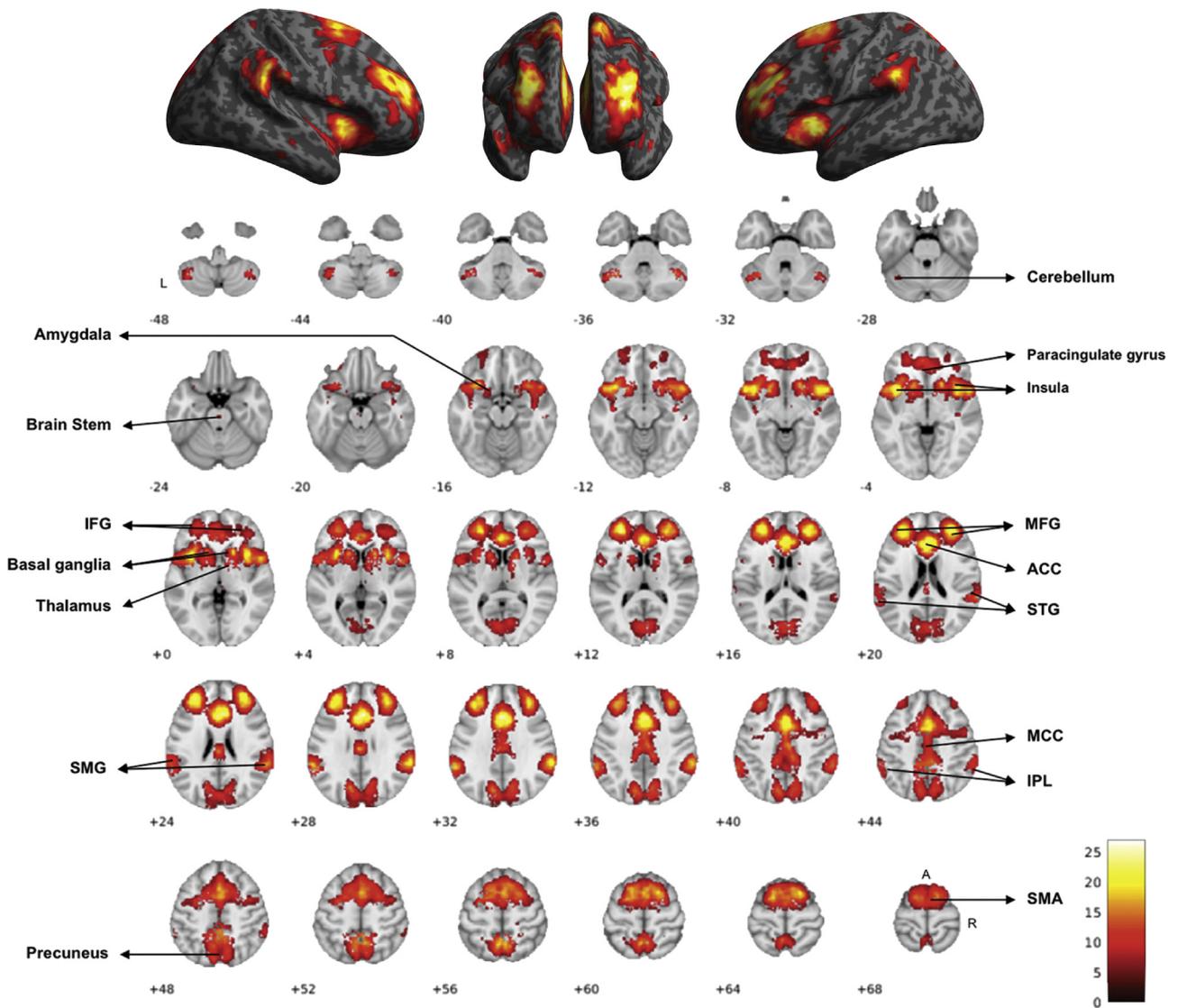
Fig. 2. Statistical parametric mapping of the cingulo-opercular network obtained with independent component analysis of resting-state fMRI data and one-sample *t*-test. Significant voxels ($p < 0.05$ FWE corrected at the cluster level) are overlaid onto an inflated cortical mesh (above) and z-axis slices of an anatomical standard MNI152 template (below). Abbreviations: ACC, anterior cingulate cortex; IFG, inferior frontal gyrus; IPL, inferior parietal lobule; MCC, middle cingulate cortex; MFG, middle frontal gyrus; SMA, supplementary motor area; SMG, supramarginal gyrus; STG, superior temporal gyrus. The color bar indicates *t* values. (For interpretation of the references to color in this figure legend, the reader is referred to the Web version of this article.)
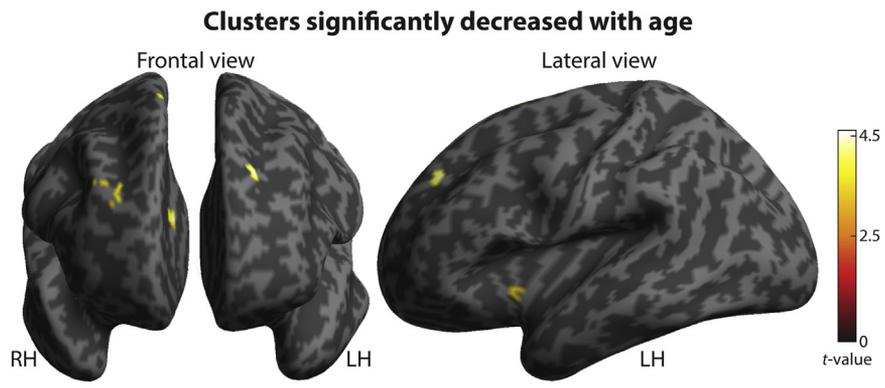

Fig. 3. SPM of voxelwise multiple regression of age on iFC in the cingulo-opercular network ($p < 0.05$ FWE corrected at the cluster level). Voxels that show significantly decreased iFC with increasing age are overlaid onto an inflated cortical mesh (light gray: gyri; dark gray: sulci). Clusters were found in the right anterior cingulate cortex and middle frontal gyrus, bilateral middle cingulate cortex, right posterior medial frontal gyrus, left superior frontal gyrus, left insula, and left cerebellum (see Table 3). Abbreviations: iFC, intrinsic functional connectivity; FWE, familywise error; LH, left hemisphere; RH, right hemisphere.

Table 3
Cingulo-opercular network clusters whose iFC significantly decreases with age

Brain region (AAL)	MNI coordinates in mm (x, y, z)	Cluster size (voxels)	Z Value of peak coordinate	p value
Right anterior cingulate cortex	2, 28, 22	166	5.14	<0.001
Left cerebellum	−50, −60, −36	141	4.58	0.001
Left insula	−44, 12, −10	93	4.53	0.011
Bilateral middle cingulate cortex	0, −18, 50	268	4.47	<0.001
Left superior frontal gyrus	−26, 40, 40	97	4.42	0.009
Right posterior medial frontal gyrus	0, 16, 64	72	4.09	0.034
Right middle frontal gyrus	26, 42, 26	66	3.81	0.046

$p < 0.05$ FWE corrected at the cluster level (height threshold $p < 0.001$ unc.). See also Fig. 3.
Key: AAL, anatomical automatic labeling; FWE, familywise error; iFC, intrinsic functional connectivity; MNI, Montreal Neurological Institute.

3.3. The iFC in the cingulo-opercular network is associated with visual processing speed C

Within the cingulo-opercular network, the iFC values of the left insula cluster correlated significantly with the visual processing speed C estimates while controlling for normalized brain volume [$r(88) = 0.33$, $p = 0.002$; Fig. 4]. None of the other clusters correlated significantly with visual processing speed C in the entire sample (all p-values > 0.244).

The iFC values of the left insular cluster were also significantly related to the time needed to complete the TMT-A [$r(87) = −0.31$, $p = 0.003$]. Furthermore, the iFC values of two other cingulo-opercular network's clusters correlated significantly with performance in the TMT-A (bilateral middle cingulate cortex: $r = −0.37$; and right posterior medial frontal gyrus: $r = −0.34$; both p-values < 0.007, Bonferroni-corrected).

3.4. Control analyses

3.4.1. Specificity of the role of the iFC in the cingulo-opercular network for visual processing speed C

For the default-mode network, age-related decreased iFC was found in the right middle temporal gyrus and the right cuneus.

However, none of these clusters' iFC values correlated significantly with visual processing speed C while controlling for brain volume (both p-values > 0.118). For the dorsal-attention network, age-related decreased iFC was found in the left superior, middle, and inferior (pars triangularis) frontal gyri, left inferior parietal lobule, left precuneus, and right middle temporal gyrus. As with the default-mode network clusters, none of the dorsal-attention network clusters' iFC values correlated significantly with visual processing speed C while controlling for brain volume (all p-values > 0.157).

To test whether the iFC of the left insula cluster was associated specifically with visual processing speed (and not generally with visual attention), we examined its correlation with VSTM capacity K and perceptual threshold t_0, controlling for brain volume. Similar to visual processing speed C, VSTM storage capacity K was significantly correlated with age, and a nonsignificant trend was also seen for the visual perceptual threshold t_0 (Table 2). However, none of the correlations between iFC in the cingulo-opercular network and these measures was significant (both p-values > 0.125), thus supporting the specificity of the association between the iFC in the cingulo-opercular network with visual processing speed. Likewise, none of the other iFC clusters of the cingulo-opercular network correlated significantly with K (all p-values > 0.355) or t_0 (all p-values > 0.202).

3.4.2. Control of potential confounds in the association between iFC in the cingulo-opercular network and visual processing speed C

Anxiety was not significantly correlated with age (both p-values > 0.073). Furthermore, the iFC of the left insula cluster did not significantly correlate with the anxiety scores derived from both STAI scales (both p-values > 0.230). Controlling for each of the anxiety scores did also not affect the correlation between visual processing speed C and the iFC of the left insula cluster (both p-values < 0.003). Similarly, controlling for possible vascular risk or gray matter density within the left insula cluster did not compromise the association between the iFC of the left insula cluster and visual processing speed C (see Supplementary Material).

3.5. The cingulo-opercular network mediates the age-related reduction in visual processing speed

Finally, we explored whether the iFC in the cingulo-opercular network mediated the association between age and visual
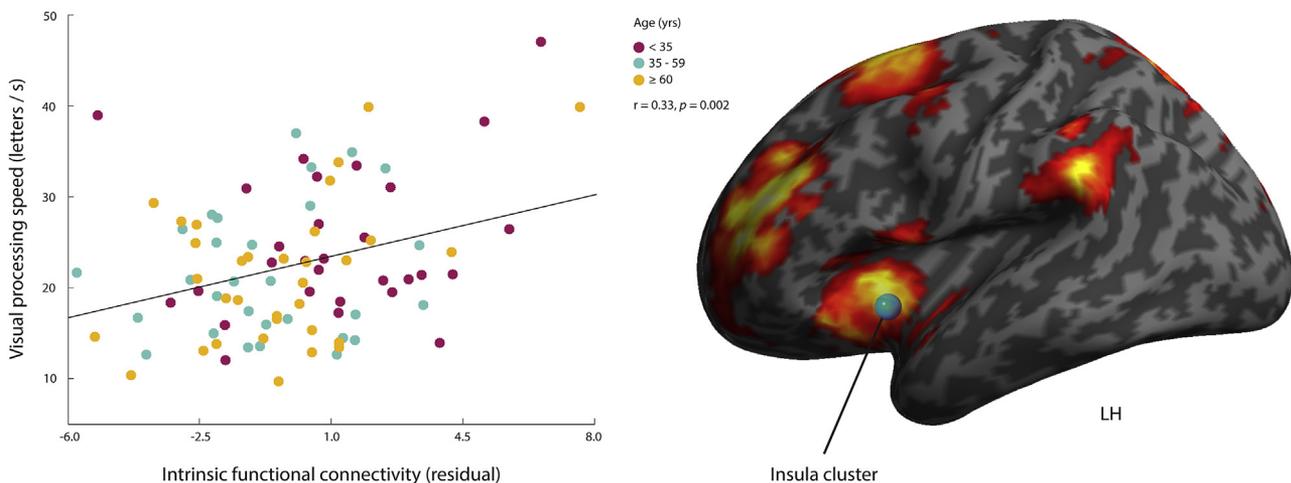

Fig. 4. Visual processing speed C as a function of the iFC in the left insula cluster of the cingulo-opercular network. The X-axis values of the scatter plot are the unstandardized residuals of the normalized brain volume regressed iFC-eigenvariate within a 5-mm radius sphere around the left insula cluster's peak: −44; 12, −10, MNI coordinates. Abbreviations: iFC, intrinsic functional connectivity; MNI, Montreal Neurological Institute.

Table 4
Bootstrap confidence intervals of potential mediators of the relationship between age and visual processing speed

Potential mediators	Indirect effect	Lower limit CI	Upper limit CI
1. Right anterior cingulate cortex	0.033	−0.015	0.086
2. Left cerebellum	0.004	−0.052	0.060
3. Left insula	**−0.091**	**−0.165**	**−0.014**
4. Bilateral middle cingulate cortex	−0.007	−0.058	0.043
5. Left superior frontal gyrus	0.015	−0.052	0.072
6. Right posterior medial frontal gyrus	0.039	−0.018	0.093
7. Right middle frontal gyrus	−0.023	−0.063	0.018
8. Normalized brain volume	−0.014	−0.084	0.063
9. Education	−0.008	−0.032	0.022
Total effect	−0.052	−0.204	0.110

The indirect effect which is significant if different from zero (in bold), as revealed by the CIs—refers to the effect of age on visual processing speed C mediated by iFC. Confidence interval (CI) level: 95% based on 10,000 bootstrap samples.

processing speed. We included all age-decreased cingulo-opercular network clusters (Table 3), along with normalized brain volume and education, as potential mediators (i.e., multiple mediation; Preacher and Hayes, 2008) of the relationship between age and visual processing speed. Table 4 lists the indirect effects (through the iFC in the cingulo-opercular network) of age on visual processing speed for each of those potential mediators and the corresponding bootstrap intervals at 95% level of confidence. In line with the partial correlation results presented in the previous section, only the left insula cluster was found to significantly mediate the association between age and visual processing speed [direct effect of age on visual processing speed: b = −0.060, standard error = 0.060, 95% confidence interval (−0.178, 0.059); see also Table 4]. Fig. 5 depicts the path model of the mediation for the left insula cluster only. This model suggests that every year of increase in age results in a decrease of 0.09 (letter per second) in visual processing speed C. Such decrease is given through the sequential effects of age on iFC in the left insula cluster (blue arrow) and of iFC in the left insula cluster on visual processing speed (red arrow).

In contrast to the TVA-based parameter of visual processing speed, as measured with whole report, neither the left insula
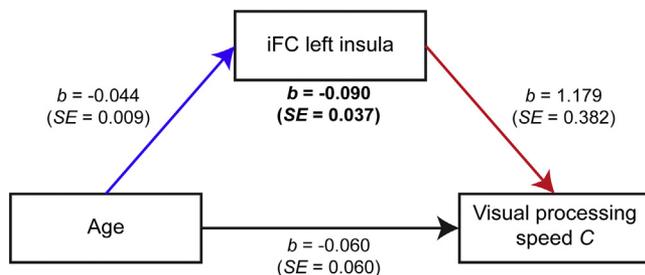

Fig. 5. Mediation model of the effect of age on visual processing speed C through the iFC in the left insula cluster of the cingulo-opercular network. This model illustrates the relationships among age, iFC in the left insula, and visual processing speed C. It presents the unstandardized coefficients (b) and standard errors (SE) of the particular effects (arrows). The blue arrow indicates a negative effect, the red arrow a positive effect, and the black arrow indicates a non-significant effect. The b and SE in bold below the "iFC left insula" is the effect of interest (i.e., effect of age on C through iFC). Abbreviation: iFC, intrinsic functional connectivity. (For interpretation of the references to color in this figure legend, the reader is referred to the Web version of this article.)

cluster of the cingulo-opercular network (indirect effect: 0.010, CI: −0.063–0.079) nor any other cluster of the cingulo-opercular network mediated the association between age and visual processing speed as measured by the TMT-A.

Control analyses were carried out to test the specificity of the relation between iFC in the cingulo-opercular network on the one hand and visual processing speed C on the other. First, testing analogous mediation models for the default mode and, respectively, the dorsal-attention network's age-relevant clusters yielded no significant results (see Supplementary Material). Second, the left insula cluster also did not mediate the association between age and VSTM capacity K (indirect effect: −0.002, CI: −0.006–0.000) or between age and visual perceptual threshold t_0 (indirect effect: 0.029, CI: −0.056–0.136).

4. Discussion

In this study, we investigated whether age-related decreases of iFC in the cingulo-opercular network are related to those in visual processing speed. First, we identified regions with age-related decrease of the iFC in the cingulo-opercular network in a group of participants of widely varying age. We found that, among these clusters, iFC in the left insula was significantly associated with a parametric, TVA-based measure of visual processing speed. This was confirmed by the results from a paper-and-pencil test of visual processing speed. Furthermore, the iFC in the respective cluster significantly mediated the effect of age on visual processing speed as measured using the TVA-based paradigm, but not as measured with the paper-and-pencil task. Taken together, our results suggest that the iFC in the cingulo-opercular network is of particular relevance for understanding visual processing speed reductions in healthy aging.

4.1. Mediator role of the iFC in the cingulo-opercular network in the visual processing speed reduction in aging

Our results (Table 2) replicate previous findings concerning decreases in both visual processing speed (Espeseth et al., 2014; Habekost et al., 2013; McAvinue et al., 2012; Salthouse, 1996; Tombaugh, 2004) and the iFC in the cingulo-opercular network (Fig. 3) (He et al., 2014; Meier et al., 2012; Onoda et al., 2012) over the course of normal aging. More importantly, they demonstrate that a decreased iFC in the cingulo-opercular network is associated with the age-related reduction in visual processing speed (Fig. 4). Specifically, the left insular iFC within the cingulo-opercular network was significantly related to visual processing speed and further found to mediate the association between age and speed (Table 4, Fig. 5). The anterior insula is a hub of the human brain (Power et al., 2013) and, in particular, an anchor of the cingulo-opercular network (e.g., Seeley et al., 2007). It plays a crucial role in allowing switching between the activity of the central executive network and of the default mode network (Sridharan et al., 2008). Accordingly, the anterior insula has also been proposed to play an integrative role between brain networks involved in external and internal processing (e.g., Menon and Uddin, 2010), permitting the individual to prepare for external or internal processing in the presence of visual stimuli (e.g., Riedl et al., 2016). A comprehensive review on the role of the anterior insula in perceptual tasks proposed that it mediates heightened alertness in sensory cortices, thus rendering the individual more sensitive to sensory stimulation (Sterzer and Kleinschmidt, 2010). In the visual domain, according to TVA (Bundesen, 1990), this would directly relate to visual processing speed. Although in line with a prominent role of the anterior insula for visual processing speed, our results should not be interpreted as indicating a specific role of a circumscribed region

within the cingulo-opercular network. Given that the insula iFC values are relative values (i.e., with respect to the other voxels of an individual's brain) within a network, we can only state that the left insula cluster *best* represented the cingulo-opercular network association with age and visual processing speed. Accordingly, we keep the interpretation of our findings at the network level.

The results of the present study are in line with previous documentations of (1) significant associations between task-evoked (Coste and Kleinschmidt, 2016; Sadaghiani and D'Esposito, 2015) and spontaneous (Sadaghiani et al., 2010; Schneider et al., 2016) fMRI BOLD activity of the cingulo-opercular network and the level of tonic alertness; of (2) a close association between tonic alertness and TVA parameter visual processing speed *C* (Bundesen et al., 2015; Finke et al., 2010; Matthias et al., 2010; Vangkilde et al., 2013); and of (3) significant differences between young participants with relatively high and relatively low visual processing speed *C* especially in the iFC in the cingulo-opercular network (Ruiz-Rizzo et al., 2018). In addition to these prior studies, we now provide evidence for the crucial role of the cingulo-opercular network for the decrease of visual processing speed across adult age. The mediating role of iFC in the cingulo-opercular network between age and visual processing speed (Table 4) suggests that it is not aging per se that, in a deterministic manner, gives rise to the well-established decrements in visual processing speed. Instead, it implies that, even at an advanced age, individuals might exhibit relatively "normal" visual processing speed (comparable to that of younger individuals), given "normal" (i.e., youth-like) iFC in the cingulo-opercular network.

We found the relationship of the iFC in the cingulo-opercular network to visual processing speed to be additionally supported by a measure that is widely used in the clinical settings for assessing processing speed: performance in the TMT-A also correlated significantly with the iFC of the left insula. In addition, other clusters, such as the middle cingulate cortex, and the posterior medial frontal gyrus correlated with performance in the TMT-A. But unlike with our TVA-derived measure of visual processing speed *C*, the association between age and performance on the TMT-A was not mediated by the iFC in any cluster within the cingulo-opercular network that showed age-related decrease in iFC. This is likely attributable to the fact that, as in most standard processing speed tasks, performance level in the TMT-A heavily relies on additional functions, such as other components of visual attention, working memory, and motor speed. As all of these functions are prone to age-related decline, age-related decrease in TMT-A performance is likely related to a relatively broad range, or more general, brain changes on the one hand. On the other, the TVA-based measure, with its high cognitive specificity is optimally suited to identifying the particular brain changes contributing to the reduction of *visual* processing speed.

Visual processing speed has long been known to explain a substantial part of the variability in different, speed-dependent cognitive tasks and fluid intelligence, especially in older adults (e.g., Deary et al., 2001, 2010; Deary and Stough, 1996). Moreover, the TVA visual processing-speed parameter *C* has been suggested to represent a quantitative measure of an individual, latent parameter (Finke et al., 2005) with substantial influence on cognitive capabilities. Our results thus indicate that the previously established links between the iFC of the left insula in the cingulo-opercular network and general cognitive measures in older adults (e.g., He et al., 2014; Onoda et al., 2012) are mediated by a reduction in this more specific, basic function.

4.2. Specificity of the association between the iFC in the cingulo-opercular network and visual processing speed

As not only the iFC in the cingulo-opercular network is known to decrease with aging, a number of control analyses were run to confirm the specificity of the relation between iFC in the cingulo-opercular network and visual processing speed. In particular, we looked at iFC in the default mode and dorsal-attention networks (Andrews-Hanna et al., 2007; Damoiseaux et al., 2008; Ferreira and Busatto, 2013). However, we found no evidence for the iFC in these two networks to contribute to the variance in visual processing speed. Thus, rather than supporting a *general* relationship between age-related decreases in iFC across diverse networks and visual processing speed decrements, our results indicate that such a relationship is particular for the iFC in the cingulo-opercular network.

Similarly, as not only visual processing speed but also other visual attention functions, such as the visual perceptual threshold and VSTM storage capacity, change with aging (Espeseth et al., 2014; McAvinue et al., 2012), we also looked at the relationship of the iFC in the cingulo-opercular network and these functions. The cognitive purity of the different measures obtained with TVA-based testing permitted us to identify a specific role for reductions in visual processing speed. Our results showed that the iFC of the cingulo-opercular network was only associated with visual processing speed *C*. Of theoretical importance, this is in line with a central assumption of the neural interpretation of TVA (Bundesen et al., 2005), namely, that the different visual attention parameters reflect distinct neural processes that contribute independently to the individual attentional performance. Thus, it is likely that the brain mechanisms underlying changes in VSTM capacity and the perceptual threshold are distinct from those in visual processing speed. Of note, as the TVA-based testing does not rely on motor speed, our results can also not be explained by age-related changes in motor performance.

Furthermore, iFC in the cingulo-opercular network is known to relate not only to cognitive measures but also to anxiety (Seeley et al., 2007). As anxiety might influence visual processing speed, as indicated, for example, by reduced processing speed *C* in patients with major depression (Gögler et al., 2017), we analyzed whether anxiety might be a critical confound in our findings. However, the STAI (trait and state) anxiety scores failed to correlate with iFC in the left insula cluster of the cingulo-opercular network.

Additional potential confounds of our results are both vascular (e.g., reactivity or pathology of the blood vessels; D'Esposito et al., 2003) and structural changes (e.g., changes in gray matter; Lu et al., 2013) that occur with aging. However, the association between iFC and visual processing speed still held while controlling for those factors. Thus, our results point to variations in the intrinsic *functional* organization of the cingulo-opercular network as critical for reductions in visual processing speed.

4.3. Limitations

Our study has a number of limitations. First, the results are based on cross-sectional and correlational data, which does not allow firm inferences to be drawn regarding the directional relationship(s) among aging, iFC, and visual processing speed. Second, the mediation analysis would need to be replicated in an independent, longitudinally assessed sample. And third, such analyses should additionally include other potential mediators derived from further brain or environmental measures. For example, it remains to be determined whether structural connectivity changes (e.g., as measured by tractography) within the cingulo-opercular network or with other networks underlie the changes in iFC.

4.4. Conclusion

Our results indicate a mediator role of the iFC in the cingulo-opercular network in the impact of aging on visual processing

speed. They thus indicate that it is not simply aging per se that, in a deterministic manner, gives rise to the well-established decrements in visual processing speed. Rather, they imply that, even at an advanced age, individuals might exhibit relatively "normal" visual processing speed (comparable to that of younger individuals), given "normal" (i.e., youth-like) iFC in the cingulo-opercular network. Future longitudinal studies could attempt to identify whether, among older individuals, changes in iFC and visual processing speed occur at similar or different time points. To conclude, the evidence presented here, for the first time, points to a significant role of the iFC in the cingulo-opercular network in the attentional processing capacity of healthy aging individuals.

Disclosure statement

The authors report no conflicts of interest.

Acknowledgements

Appendix A. Supplementary data

Supplementary data related to this article can be found, in the online version, at https://doi.org/10.1016/j.neurobiolaging.2018.09.014.

References

Allen, E.A., Erhardt, E.B., Damaraju, E., Gruner, W., Segall, J.M., Silva, R.F., Havlicek, M., Rachakonda, S., Fries, J., Kalyanam, R., Michael, A.M., Caprihan, A., Turner, J.A., Eichele, T., Adelsheim, S., Bryan, A.D., Bustillo, J., Clark, V.P., Feldstein Ewing, S.W., Filbey, F., Ford, C.C., Hutchison, K., Jung, R.E., Kiehl, K.A., Kodituwakku, P., Komesu, Y.M., Mayer, A.R., Pearlson, G.D., Phillips, J.P., Sadek, J.R., Stevens, M., Teuscher, U., Thoma, R.J., Calhoun, V.D., 2011. A baseline for the multivariate comparison of resting-state networks. Front Syst Neurosci 5, 2.

Andrews-Hanna, J.R., Snyder, A.Z., Vincent, J.L., Lustig, C., Head, D., Raichle, M.E., Buckner, R.L., 2007. Disruption of large-scale brain systems in advanced aging. Neuron 56, 924–935.

Barnes, L.L., Harp, D., Jung, W.S., 2002. Reliability generalization of scores on the Spielberger state-trait anxiety inventory. Educ. Psychol. Meas. 62, 603–618.

Beck, A.T., Steer, R.A., Brown, G.K., 1996. Manual for the Beck Depression Inventory-ii, second ed. The Psychological Corporation, San Antonio, TX.

Beckmann, C.F., Mackay, C.E., Filippini, N., Smith, S., 2009. Group comparison of resting-state FMRI data using multi-subject ICA and dual regression. Neuroimage 47 (Suppl 1), S148.

Beckmann, C.F., Smith, S.M., 2004. Probabilistic independent component analysis for functional magnetic resonance imaging. IEEE Trans. Med. Imaging 23, 137–152.

Bublak, P., Redel, P., Sorg, C., Kurz, A., Forstl, H., Muller, H.J., Schneider, W.X., Finke, K., 2011. Staged decline of visual processing capacity in mild cognitive impairment and Alzheimer's disease. Neurobiol. Aging 32, 1219–1230.

Bundesen, C., 1990. A theory of visual attention. Psychol. Rev. 97, 523–547.

Bundesen, C., Habekost, T., Kyllingsbaek, S., 2005. A neural theory of visual attention: bridging cognition and neurophysiology. Psychol. Rev. 112, 291–328.

Bundesen, C., Vangkilde, S., Petersen, A., 2015. Recent developments in a computational theory of visual attention (TVA). Vis. Res 116 (Pt B), 210–218.

Chao-Gan, Y., Yu-Feng, Z., 2010. DPARSF: a MATLAB toolbox for "Pipeline" data analysis of resting-state fMRI. Front. Syst. Neurosci. 4, 13.

Coste, C.P., Kleinschmidt, A., 2016. Cingulo-opercular network activity maintains alertness. Neuroimage 128, 264–272.

D'Esposito, M., Deouell, L.Y., Gazzaley, A., 2003. Alterations in the BOLD fMRI signal with ageing and disease: a challenge for neuroimaging. Nat. Rev. Neurosci. 4, 863–872.

Damoiseaux, J.S., Beckmann, C.F., Arigita, E.J., Barkhof, F., Scheltens, P., Stam, C.J., Smith, S.M., Rombouts, S.A., 2008. Reduced resting-state brain activity in the "default network" in normal aging. Cereb. Cortex 18, 1856–1864.

De Luca, M., Beckmann, C.F., De Stefano, N., Matthews, P.M., Smith, S.M., 2006. fMRI resting state networks define distinct modes of long-distance interactions in the human brain. Neuroimage 29, 1359–1367.

Deary, I.J., Der, G., Ford, G., 2001. Reaction times and intelligence differences: a population-based cohort study. Intelligence 29, 389–399.

Deary, I.J., Johnson, W., Starr, J.M., 2010. Are processing speed tasks biomarkers of cognitive aging? Psychol. Aging 25, 219–228.

Deary, I.J., Stough, C., 1996. Intelligence and inspection time: achievements, prospects, and problems. Am. Psychol. 51, 599–608.

Dosenbach, N.U., Fair, D.A., Cohen, A.L., Schlaggar, B.L., Petersen, S.E., 2008. A dual-networks architecture of top-down control. Trends Cogn. Sci. 12, 99–105.

Dosenbach, N.U., Fair, D.A., Miezin, F.M., Cohen, A.L., Wenger, K.K., Dosenbach, R.A., Fox, M.D., Snyder, A.Z., Vincent, J.L., Raichle, M.E., Schlaggar, B.L., Petersen, S.E., 2007. Distinct brain networks for adaptive and stable task control in humans. Proc. Natl. Acad. Sci. U S A. 104, 11073–11078.

Dyrholm, M., Kyllingsbaek, S., Espeseth, T., Bundesen, C., 2011. Generalizing parametric models by introducing trial-by-trial parameter variability: the case of TVA. J. Math. Psychol. 55, 416–429.

Espeseth, T., Vangkilde, S.A., Petersen, A., Dyrholm, M., Westlye, L.T., 2014. TVA-based assessment of attentional capacities-associations with age and indices of brain white matter microstructure. Front Psychol. 5, 1177.

Feinberg, D.A., Setsompop, K., 2013. Ultra-fast MRI of the human brain with simultaneous multi-slice imaging. J. Magn. Reson. 229, 90–100.

Ferreira, L.K., Busatto, G.F., 2013. Resting-state functional connectivity in normal brain aging. Neurosci. Biobehav Rev. 37, 384–400.

Filippini, N., MacIntosh, B.J., Hough, M.G., Goodwin, G.M., Frisoni, G.B., Smith, S.M., Matthews, P.M., Beckmann, C.F., Mackay, C.E., 2009. Distinct patterns of brain activity in young carriers of the APOE-epsilon4 allele. Proc. Natl. Acad. Sci. U S A. 106, 7209–7214.

Finke, K., Bublak, P., Krummenacher, J., Kyllingsbaek, S., Muller, H.J., Schneider, W.X., 2005. Usability of a theory of visual attention (TVA) for parameter-based measurement of attention I: evidence from normal subjects. J. Int. Neuropsychol. Soc. 11, 832–842.

Finke, K., Dodds, C.M., Bublak, P., Regenthal, R., Baumann, F., Manly, T., Muller, U., 2010. Effects of modafinil and methylphenidate on visual attention capacity: a TVA-based study. Psychopharmacology (Berl) 210, 317–329.

Folstein, M.F., Folstein, S.E., McHugh, P.R., 1975. "Mini-mental state". A practical method for grading the cognitive state of patients for the clinician. J. Psychiatr. Res. 12, 189–198.

Fox, M.D., Raichle, M.E., 2007. Spontaneous fluctuations in brain activity observed with functional magnetic resonance imaging. Nat. Rev. Neurosci. 8, 700–711.

Gögler, N., Willacker, L., Funk, J., Strube, W., Langgartner, S., Napiorkowski, N., Hasan, A., Finke, K., 2017. Single-session transcranial direct current stimulation induces enduring enhancement of visual processing speed in patients with major depression. Eur. Arch. Psychiatry Clin. Neurosci. 267, 671–686.

Habekost, T., Petersen, A., Vangkilde, S., 2014. Testing attention: comparing the ANT with TVA-based assessment. Behav. Res. Methods 46, 81–94.

Habekost, T., Vogel, A., Rostrup, E., Bundesen, C., Kyllingsbaek, S., Garde, E., Ryberg, C., Waldemar, G., 2013. Visual processing speed in old age. Scand. J. Psychol. 54, 89–94.

Hayes, A.F., 2012. PROCESS: A Versatile Computational Tool for Observed Variable Mediation, Moderation, and Conditional Process Modeling. In: http://www.afhayes.com/public/process2012.pdf. Accessed December 4, 2017.

Hayes, A.F., Rockwood, N.J., 2017. Regression-based statistical mediation and moderation analysis in clinical research: observations, recommendations, and implementation. Behav. Res. Ther. 98, 39–57.

He, X., Qin, W., Liu, Y., Zhang, X., Duan, Y., Song, J., Li, K., Jiang, T., Yu, C., 2014. Abnormal salience network in normal aging and in amnestic mild cognitive impairment and Alzheimer's disease. Hum. Brain Mapp. 35, 3446–3464.

Hyvarinen, A., 1999. Fast and robust fixed-point algorithms for independent component analysis. IEEE Trans. Neural Netw. 10, 626–634.

Kyllingsbaek, S., 2006. Modeling visual attention. Behav. Res. Methods 38, 123–133.

Laux, L., Glanzmann, P., Schaffner, P., Spielberger, C.D., 1981. Das State-Trait-Angstinventar (Testmappe mit Handanweisung, Fragebogen STAI-G Form X 1 und Fragebogen STAI-G Form X 2). Beltz, Weinheim.

Lu, P.H., Lee, G.J., Tishler, T.A., Meghpara, M., Thompson, P.M., Bartzokis, G., 2013. Myelin breakdown mediates age-related slowing in cognitive processing speed in healthy elderly men. Brain Cogn. 81, 131–138.

Mackinnon, D.P., Fairchild, A.J., 2009. Current directions in mediation analysis. Curr. Dir. Psychol. Sci. 18, 16.

Matthias, E., Bublak, P., Muller, H.J., Schneider, W.X., Krummenacher, J., Finke, K., 2010. The influence of alertness on spatial and nonspatial components of visual attention. J. Exp. Psychol. Hum. Percept Perform 36 (1), 38–56.

McAvinue, L.P., Habekost, T., Johnson, K.A., Kyllingsbaek, S., Vangkilde, S., Bundesen, C., Robertson, I.H., 2012. Sustained attention, attentional selectivity, and attentional capacity across the lifespan. Atten. Percept. Psychophys. 74 (8), 1570–1582.

Meier, T.B., Desphande, A.S., Vergun, S., Nair, V.A., Song, J., Biswal, B.B., Meyerand, M.E., Birn, R.M., Prabhakaran, V., 2012. Support vector machine classification and characterization of age-related reorganization of functional brain networks. Neuroimage 60, 601–613.

Menon, V., Uddin, L.Q., 2010. Saliency, switching, attention and control: a network model of insula function. Brain Struct. Funct. 214, 655–667.

Murphy, K., Bodurka, J., Bandettini, P.A., 2007. How long to scan? The relationship between fMRI temporal signal to noise ratio and necessary scan duration. Neuroimage 34, 565–574.

Nickerson, L.D., Smith, S.M., Ongur, D., Beckmann, C.F., 2017. Using dual regression to investigate network shape and amplitude in functional connectivity analyses. Front Neurosci. 11, 115.

Onoda, K., Ishihara, M., Yamaguchi, S., 2012. Decreased functional connectivity by aging is associated with cognitive decline. J. Cogn. Neurosci. 24, 2186—2198.

Posner, M.I., Petersen, S.E., 1990. The attention system of the human brain. Annu. Rev. Neurosci. 13, 25—42.

Power, J.D., Barnes, K.A., Snyder, A.Z., Schlaggar, B.L., Petersen, S.E., 2012. Spurious but systematic correlations in functional connectivity MRI networks arise from subject motion. Neuroimage 59, 2142—2154.

Power, J.D., Schlaggar, B.L., Lessov-Schlaggar, C.N., Petersen, S.E., 2013. Evidence for hubs in human functional brain networks. Neuron 79, 798—813.

Preacher, K.J., Hayes, A.F., 2004. SPSS and SAS procedures for estimating indirect effects in simple mediation models. Behav. Res. Methods Instrum Comput. 36, 717—731.

Preacher, K.J., Hayes, A.F., 2008. Asymptotic and resampling strategies for assessing and comparing indirect effects in multiple mediator models. Behav. Res. Methods 40, 879—891.

Preibisch, C., Castrillon, G.J., Buhrer, M., Riedl, V., 2015. Evaluation of multiband EPI acquisitions for resting state fMRI. PLoS One 10, e0136961.

Raichle, M.E., 2015. The restless brain: how intrinsic activity organizes brain function. Philos. Trans. R. Soc. Lond. B Biol. Sci. 370, 20140172.

Reitan, R.M., Wolfson, D., 1985. The Halstead-reitan Neuropsychological Test Battery: Therapy and Clinical Interpretation. Neuropsychological Press, Tucson, AZ.

Riedl, V., Utz, L., Castrillon, G., Grimmer, T., Rauschecker, J.P., Ploner, M., Friston, K.J., Drzezga, A., Sorg, C., 2016. Metabolic connectivity mapping reveals effective connectivity in the resting human brain. Proc Natl Acad Sci U S A 113, 428—433.

Ruiz-Rizzo, A.L., Bublak, P., Redel, P., Grimmer, T., Muller, H.J., Sorg, C., Finke, K., 2017. Simultaneous object perception deficits are related to reduced visual processing speed in amnestic mild cognitive impairment. Neurobiol. Aging 55, 132—142.

Ruiz-Rizzo, A.L., Neitzel, J., Muller, H.J., Sorg, C., Finke, K., 2018. Distinctive correspondence between separable visual attention functions and intrinsic brain networks. Front. Hum. Neurosci. 12, 89.

Sadaghiani, S., D'Esposito, M., 2015. Functional characterization of the cingulo-opercular network in the maintenance of tonic alertness. Cereb. Cortex 25, 2763—2773.

Sadaghiani, S., Scheeringa, R., Lehongre, K., Morillon, B., Giraud, A.L., Kleinschmidt, A., 2010. Intrinsic connectivity networks, alpha oscillations, and tonic alertness: a simultaneous electroencephalography/functional magnetic resonance imaging study. J. Neurosci. 30, 10243—10250.

Salthouse, T.A., 1996. The processing-speed theory of adult age differences in cognition. Psychol. Rev. 103, 403—428.

Schneider, M., Hathway, P., Leuchs, L., Samann, P.G., Czisch, M., Spoormaker, V.I., 2016. Spontaneous pupil dilations during the resting state are associated with activation of the salience network. Neuroimage 139, 189—201.

Seeley, W.W., Menon, V., Schatzberg, A.F., Keller, J., Glover, G.H., Kenna, H., Reiss, A.L., Greicius, M.D., 2007. Dissociable intrinsic connectivity networks for salience processing and executive control. J. Neurosci. 27, 2349—2356.

Sestieri, C., Corbetta, M., Spadone, S., Romani, G.L., Shulman, G.L., 2014. Domain-general signals in the cingulo-opercular network for visuospatial attention and episodic memory. J. Cogn. Neurosci. 26, 551—568.

Smith, D.V., Utevsky, A.V., Bland, A.R., Clement, N., Clithero, J.A., Harsch, A.E., McKell Carter, R., Huettel, S.A., 2014. Characterizing individual differences in functional connectivity using dual-regression and seed-based approaches. Neuroimage 95, 1—12.

Smith, S.M., Fox, P.T., Miller, K.L., Glahn, D.C., Fox, P.M., Mackay, C.E., Filippini, N., Watkins, K.E., Toro, R., Laird, A.R., Beckmann, C.F., 2009. Correspondence of the brain's functional architecture during activation and rest. Proc. Natl. Acad. Sci. U S A. 106, 13040—13045.

Smith, S.M., Jenkinson, M., Woolrich, M.W., Beckmann, C.F., Behrens, T.E., Johansen-Berg, H., Bannister, P.R., De Luca, M., Drobnjak, I., Flitney, D.E., Niazy, R.K., Saunders, J., Vickers, J., Zhang, Y., De Stefano, N., Brady, J.M., Matthews, P.M., 2004. Advances in functional and structural MR image analysis and implementation as FSL. Neuroimage 23 (Suppl 1), S208—S219.

Smith, S.M., Zhang, Y., Jenkinson, M., Chen, J., Matthews, P.M., Federico, A., De Stefano, N., 2002. Accurate, robust, and automated longitudinal and cross-sectional brain change analysis. Neuroimage 17, 479—489.

Sperling, G., 1960. The information available in brief visual presentations. Psychol. Monogr. Gen. Appl. 74, 1—29.

Spielberger, C.D., Gorsuch, R.L., Lushene, R.E., 1970. State-trait Anxiety Inventory, Manual for the State-trait Anxiety Inventory. Consulting Psychologist Press, Palo Alto, CA.

Sridharan, D., Levitin, D.J., Menon, V., 2008. A critical role for the right fronto-insular cortex in switching between central-executive and default-mode networks. Proc. Natl. Acad. Sci. U S A. 105, 12569—12574.

Sterzer, P., Kleinschmidt, A., 2010. Anterior insula activations in perceptual paradigms: often observed but barely understood. Brain Struct Funct 214, 611—622.

Sturm, W., Willmes, K., 2001. On the functional neuroanatomy of intrinsic and phasic alertness. Neuroimage 14 (1 Pt 2), S76—S84.

Tombaugh, T.N., 2004. Trail Making Test A and B: normative data stratified by age and education. Arch. Clin. Neuropsychol. 19, 203—214.

Vangkilde, S., Petersen, A., Bundesen, C., 2013. Temporal expectancy in the context of a theory of visual attention. Philos. Trans. R. Soc. Lond. B Biol. Sci. 368, 20130054.

Weintraub, S., Salmon, D., Mercaldo, N., Ferris, S., Graff-Radford, N.R., Chui, H., Cummings, J., DeCarli, C., Foster, N.L., Galasko, D., Peskind, E., Dietrich, W., Beekly, D.L., Kukull, W.A., Morris, J.C., 2009. The Alzheimer's disease centers' uniform data set (UDS): the neuropsychologic test battery. Alzheimer Dis. Assoc. Disord. 23, 91—101.

Wiegand, I., Tollner, T., Dyrholm, M., Muller, H.J., Bundesen, C., Finke, K., 2014. Neural correlates of age-related decline and compensation in visual attention capacity. Neurobiol. Aging 35, 2161—2173.

Yeo, B.T., Krienen, F.M., Sepulcre, J., Sabuncu, M.R., Lashkari, D., Hollinshead, M., Roffman, J.L., Smoller, J.W., Zollei, L., Polimeni, J.R., Fischl, B., Liu, H., Buckner, R.L., 2011. The organization of the human cerebral cortex estimated by intrinsic functional connectivity. J. Neurophysiol. 106, 1125—1165.